Fast Oxygen Reduction Catalyzed by a Copper(II) Tris(2-pyridylmethyl)amine Complex via a Mononuclear Stepwise Mechanism

Michiel Langerman,[a] and Dennis. G. H. Hetterscheid*[a]

Abstract: *Catalytic pathways for the reduction of dioxygen can either lead to the formation of water or peroxide as the reaction product. We demonstrate that the electrocatalytic reduction of O_2 by the pyridylalkylamine copper complex $[Cu(tmpa)(L)]^{2+}$ in neutral aqueous solution follows a stepwise $4e^-/4H^+$ pathway, in which H_2O_2 is formed as a detectable intermediate and subsequently reduced to H_2O in two separate catalytic reactions. Additionally, these homogeneous catalytic reactions are shown to be first order in catalyst concentration. Coordination of O_2 to Cu^I is found to be the rate determining step in the formation of the peroxide intermediate. Furthermore, the electrochemical study of the reaction kinetics reveals a high turnover frequency of 1.5×10^5 s^{-1}, the highest reported for any molecular copper catalyst.*

With the shift in the energy landscape from fossil fuels towards sustainable sources of energy, storage and conversion of fuels such as hydrogen is expected to play an important role. It is therefore important that efficient fuel cells are available to minimize energy loss during the fuel-to-energy interconversion. However, the cathodic oxygen reduction reaction (ORR) is a significant limiting factor in the efficiency of fuel cells. In nature, multicopper oxidases such as laccase are known to be able to catalyze the four-electron reduction of O_2 to H_2O efficiently.[2] Immobilization of Laccase on electrodes has shown that the ORR can be performed close to the thermodynamic equilibrium potential of water.[3] Mimics for the active site these copper enzymes may allow for the elucidation of the catalytic mechanism of the ORR, and a wide range of model copper systems have been studied for their oxygen activation reactivity.[4] While some early examples of copper complexes have been studied for their activity towards the ORR[5], only in the last decade have the first molecular copper model catalysts been evaluated for their ORR activity, either by means of sacrificial reductants or via electrochemical studies.[6] $[Cu(tmpa)(L)]^{2+}$ (tmpa = tris(2-pyridylmethyl)amine, L = solvent) and many derivatives of the pyridylalkylamine template have been studied as a mimic for active sites in redox active metalloenzymes for its non-planar and flexible coordination sphere and its reactivity towards dioxygen.[4e, 7] The dioxygen binding chemistry of Cu-tmpa has been thoroughly studied by Karlin *et al.*[8] It was shown that in a range of solvents, the binding of dioxygen to Cu^I(tmpa) leads fast formation of an end-on Cu^{II} superoxo complex, followed by a slower dimerization step to form a dinuclear copper peroxo complex. Additionally, Fukuzumi and Karlin have studied the ORR activity of Cu-tmpa in acetone, using decamethylferrocene as a sacrificial reductant, which was shown to involve a dinuclear intermediate.[6a, 6d] Recently, it was also shown that Cu-tmpa, and several derivatives, adsorbed on carbon black catalyze the electrochemical ORR in aqueous buffer solutions.[9] The ORR activity of Cu-tmpa in solution was also investigated, as well as pH effects on the redox chemistry.[10] However, thus far catalytic rates have not been reported and the mechanism wherein ORR occurs has not been solved.

In this study we have established that Cu-tmpa is a very fast homogeneous electrocatalyst for the ORR in neutral aqueous solution. Additionally, a comprehensive study of the product formation using R(R)DE techniques has provided important new insight into the electrocatalytic ORR mechanism, and show that catalysis occurs at a single copper site via a stepwise mechanism.

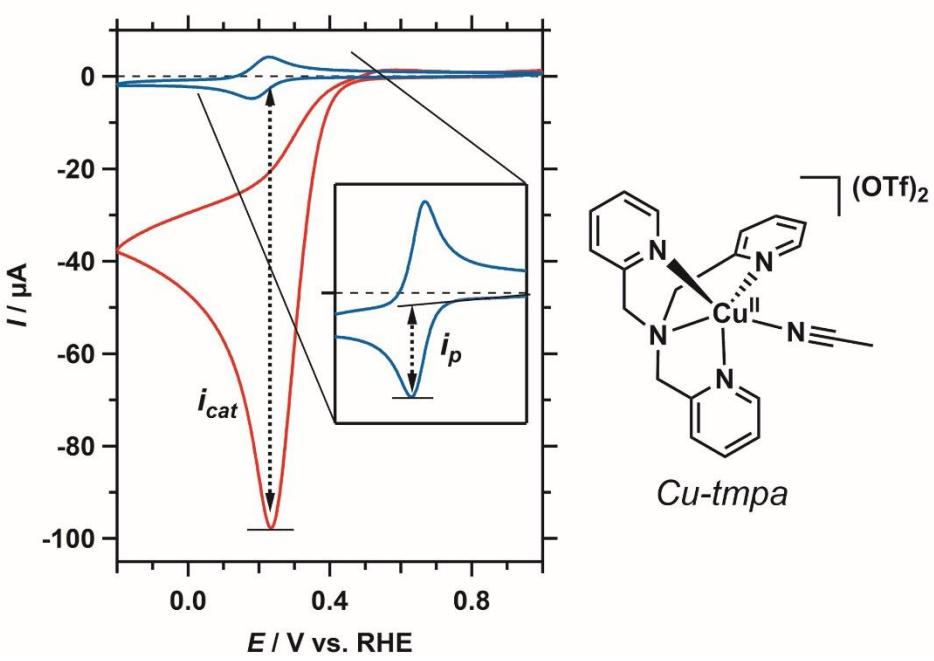

Figure 1. CVs of 0.32 mM Cu-tmpa in the presence of 1 atm Ar (blue, zoom in inset) or 1 atm O_2 (red). $E_{cat/2}$ = 0.31 V vs. RHE. Conditions: pH 7 phosphate buffer ([PO_4] = 100 mM), 1 atm O_2, 293K, 100 mV/s scan rate.

The redox and catalytic behavior of Cu-tmpa in a phosphate buffer (PB) solution at pH 7, containing 100 mM phosphate salts (NaH_2PO_4 and Na_2HPO_4), was investigated. Cyclic voltammograms (CVs) of Cu-tmpa were recorded using a Glassy Carbon (GC) working electrode (A = 0.0707 cm^2). In the presence of 1 atm argon, a well-defined reversible Cu^{I}/Cu^{II} redox couple is visible at $E_{1/2}$ = 0.21 V vs. RHE, shown in Figure 1. . In the presence of 1 atm O_2, a peak-shaped catalytic wave appears with an onset potential at 0.5 V vs. RHE. The peak-shaped catalytic wave is characteristic for cases of substrate depletion, demonstrating the very fast catalysis by Cu-tmpa. Electrochemical quartz crystal microbalance (EQCM) experiments established the homogeneity of the catalyst both under non-catalytic and catalytic conditions (see SI section 2.3).[13]

Determination of the relationship between the catalytic current and the catalyst concentration would provide useful insight towards the possible mechanism for the ORR. By measuring CVs in the presence of 1 atm O_2 at low catalyst concentrations in the range between 0.1 and 1.0 µM Cu-tmpa, a linear first-order dependence of the catalytic current on the catalyst concentration was observed (Figure S5).

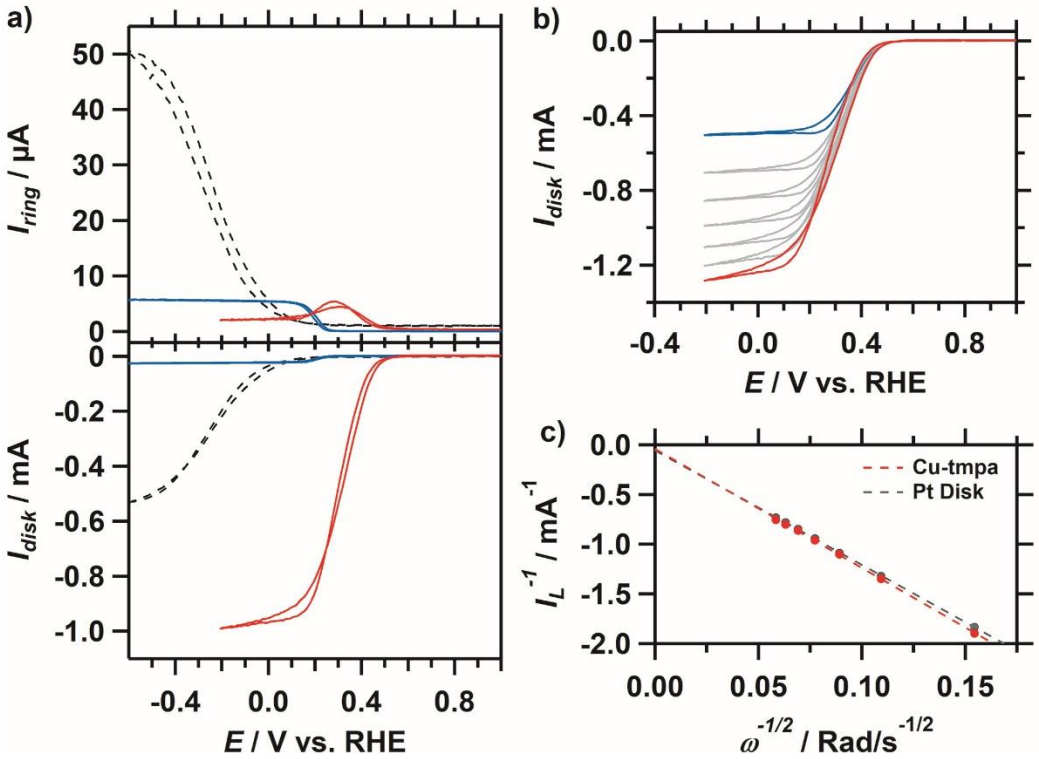

Figure 2. a) RRDE CVs of bare GC (dotted line) under 1 atm O_2 and Cu-tmpa (0.3 mM) under 1 atm Ar (blue) and 1 atm O_2 (red) at 1600 RPM. b) Disk current of Cu-tmpa (0.3 mM) under 1 atm O_2 at different rotation rates from 400 RPM (blue line) to 2800 RPM (red line); 400 RPM increments. c) Koutecky-Levich plot of the inverse limiting current (I_L^{-1}) at -0.2 V (vs. RHE.) as a function of the inverse square root of the rotation rate. Conditions: pH 7 PB ([PO_4] = 100 mM), 293K, Pt ring at 1.2 V vs. RHE, 50 mV/s scan rate.

To determine product selectivity and the electron transfer number of the catalyst in neutral aqueous solution rotating (ring-) disk electrode (R(R)DE) voltammetry was used. Previous hydrodynamic studies on the electrocatalytic ORR performance of Cu-tmpa have been either carried out by using a Vulcan supported surface deposit of Cu-tmpa[9], or have only evaluated the behavior of Cu-tmpa in aqueous solution under non-catalytic conditions.[10b] While R(R)DE voltammetry is mostly used to study heterogeneous catalytic reactions, it can be used to study homogeneous catalytic reactions under certain conditions. One of the main difficulties with the use of the R(R)DE methods for homogeneous catalysts is that both the product and substrate are present in the liquid phase. For complex multi-electron multi-step catalytic reactions (ECE, or ECEC') such as the ORR, this can result from significant deviations from the behavior dictated by the Koutecky-Levich (KL) equation, which governs the behavior of reactions with one diffusing species. In such cases, slow catalysis will result in non-ideal behavior of the measured limiting currents as a function of the rotation rate, and deviations from linearity will be observed in KL-plots. However, for fast catalytic reactions, the limiting current corresponds to the electron transfer number (*n*) of the catalytic reaction.[14] In effect, sufficiently fast molecular catalysts (where k >> rotation rate) can be considered to behave as heterogeneous within this time frame. Indeed, this is exactly what

is observed in the case of Cu-tmpa. Figure 2A shows a clear positive shift in the ORR onset potential to 0.5 V vs. RHE in the presence of Cu-tmpa compared to the bare GC electrode. KL analysis was performed on the mass-transport limiting current (I_L) obtained at different rotation rates (Figure 2B/C). Indeed, good linearity is achieved in the KL-plot, similar to that of a Pt disk electrode. This shows that *n* is constant as a function of rotation rate under these conditions. The number of electrons involved in the homogeneous ORR catalyzed by Cu-tmpa was determined to be 3.9 (see SI section 2.5), which shows the high selectivity towards the 4-electron reduction of dioxygen. This selectivity is in agreement with the heterogenized carbon black supported Cu-tmpa system.[9b]

For product determination on the ring, it is also important to account for any contributions from reduced catalytic intermediate species towards the observed ring current, as these species could also be oxidized at the ring. A small oxidative ring current can be seen from 0.5 to 0.1 V vs RHE during catalysis, which disappears as the mass-transport limited current is reached (Figure 2A, red trace). A thorough analysis showed that this can be attributed to H_2O_2 oxidation (SI section 2.5).

At the onset of the catalytic activity, significant amounts of H_2O_2 are detected, both for catalyst concentrations of 0.3 mM (~75%) and 1.0 µM (~90%) (Figure 3). A plateau of $\%H_2O_2$ is clearly visible for the lower concentration, while this is less pronounced for the higher catalyst concentration. These percentages decrease with decreasing potential and upon reaching the limiting current potential regime the $\%H_2O_2$ stabilizes at 4% and 20% at 0.0 V vs. RHE for 0.3 mM and 1.0 µM Cu-tmpa, respectively. However, below 0.1 V a contribution of the GC electrode towards H_2O_2 production cannot be excluded. These results show that a catalytic reaction that leads to the formation H_2O_2 is active over the entire potential window.

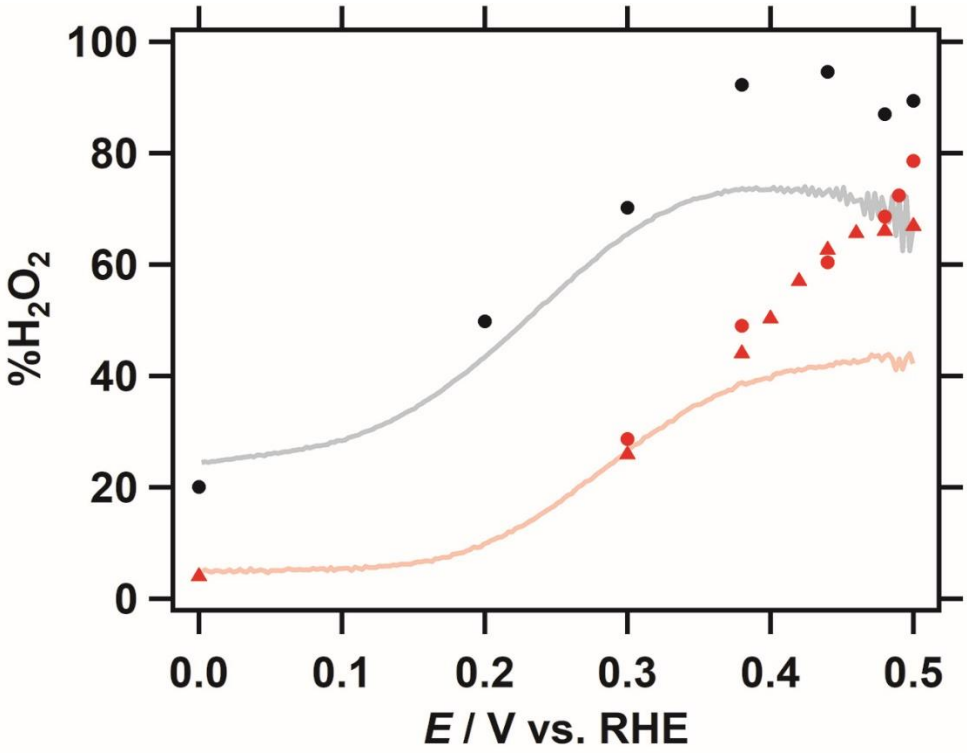

Figure 3. $\%H_2O_2$ obtained from RRDE CA (dots and triangles) and LSV (lines, 50 mV/s) measurements as a function of applied potential at a rotation rate of 1600 RPM with 0.3 mM (red), and 1.0 µM (black) Cu-tmpa present. Conditions: pH 7 PB ($[PO_4]$ = 100 mM), 293K, Pt ring at 1.2 V vs. RHE.

Conversion of i_{disk} measured during RDE experiments to the kinetic current density (j_k) allows for the evaluation of Tafel slopes of the ORR in the potential region where the current is not mass-transport limited. By plotting the applied potential as a function of the logarithm of j_k a Tafel plot can be made. Figure 4. In the presence of O_2, a clear change of Tafel slope from is seen around 0.38 V vs. RHE, while in the presence of H_2O_2 under the exact same conditions no change in slope is observed. The observed slope change during ORR indicates that a different process becomes rate-determining. The potential at which this occurs closely matches the potential where half the limiting current is observed and is below the onset potential The Tafel slope observed for the reduction of H_2O_2 by Cu-tmpa is very close to the -136 mV/dec slope observed between 0.38 V and 0.20 V during the ORR, which indicates that the same step in the mechanism is rate-determining in this regime. Tafel slopes derived from measurements performed at low (1.0 µM) catalyst concentration show the same behaviour as at higher Cu-tmpa concentration (Figure S15).

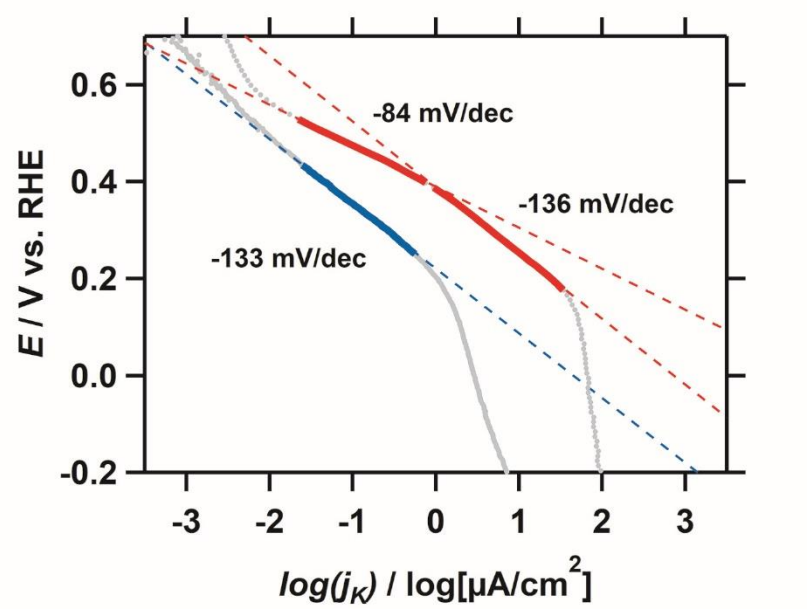

Figure 4. Plot of Tafel slopes derived from RRDE CV at 1600 RPM in the presence of 1 atm O_2 (red lines) or 1.1 mM H_2O_2 (blue line). Conditions: pH 7 PB ([PO_4] = 100 mM), [Cu-tmpa] = 0.3 mM, 293K, 50 mV/s scan rate.

Turnover frequencies (TOFs ,s^{-1}) were obtained from electrochemical measurements; either by direct determination using the catalytic current enhancement;[11b] or by applying the foot-of-the-wave analysis (FOWA)..[11a, 11d, 12a, 12b] FOWA is not affected by side phenomena such as substrate consumption, catalyst deactivation, or product inhibition and therefore especially useful for the ORR, where substrate consumption plays an important role. If more reliable kinetic conditions can be achieved during catalysis, the observed first order rate constant k_{obs} (or TOF) for the ORR can be directly determined from the catalytic current enhancement (i_{cat}/i_p) by applying Eq. 3.

$$\frac{i_{cat}}{i_p} = 2.24n\sqrt{\frac{RT}{Fv}k_{obs}} \qquad (3)$$

Here i_{cat} and i_p refer to the maximum catalytic current and the peak reductive current of the $Cu^{(II/I)}$ redox couple, respectively (Figure 1).[11b] From the current enhancement derived at low catalyst concentration (0.1-1.0 µM), a TOF of $1.5\times10^5 \pm 0.2\times10^5$ s^{-1} was obtained (SI section 2.10, Figure S16). It is important to note that this TOF is associated with the overall 4e catalytic reaction. However, as shown by the RRDE measurements and Tafel slope analysis, there are two different rate-determining catalytic regimes. Interestingly, FOWA can be employed to determine the k_{obs} (or TOF_{max}) associated with the partial reduction of O_2 to H_2O_2, as FOWA only uses the foot of

the catalytic wave where H_2O_2 reduction rates are still negligibleThe TOF_{max} for Cu-tmpa in pH 7 phosphate buffer in the presence of 1 atm O_2 was found to be $1.8\times10^6 \pm 0.6\times10^6$ s^{-1}.

It has been firmly established by stop flow experiments that oxygen binding to $[Cu(tmpa)]^+$ proceeds via a fast equilibrium to initially produce $[Cu^{II}(O_2^{\bullet-})(tmpa)]^+$ as a detectable intermediate.[8b] This species subsequently forms the $[\{Cu^{II}(tmpa)\text{-}_2(\mu\text{-}O_2)]^{2+}$ dimer in a reaction that is consistently slower than the initial oxygen binding over a wide temperature and solvent range. If catalysis were to proceed via such a dimeric species, it should lead to a second order dependence in Cu-tmpa. Instead, the observed linearity in the FOWA region is in agreement with a catalytic first order relationship in catalyst,[12a] and is in good agreement with the first order catalyst concentration dependence discussed previously. That catalysis can indeed occur at a single site copper species was demonstrated previously using a site isolated immobilized copper phenanthroline system, albeit with very low catalytic conversion to H_2O_2.[6b]

The TOF_{max} associated with the first 2 $e^-/2H^+$ reduction step to H_2O_2 is the same, within the error margin, as the TOFs (also determined by FOWA) of the fastest iron porphyrin complexes (2.2×10^6 s^{-1}) recently reported by Mayer *et al.*, which are the fastest homogeneous ORR catalysts in acetonitrile reported to date.[6e, 15] When accounting for the oxygen solubility difference using $TOF = k_{O2}[O_2]$, where $[O_2] \approx 1.1$ mM in water ($[PO_4]$= 100 mM) under 1 atm O_2, the obtained second order rate constant $k_{O2} = 1.6\times10^9 (\pm 0.5\times10^9)$ M^{-1} s^{-1} is an order of magnitude faster than the aforementioned iron porphyrins. This k_{O2} is comparable to the second order rate constant of O_2 binding, $k_{O2} = 1.3\times10^9$ M^{-1} s^{-1}, found for Cu^I-tmpa in THF, which represents the fastest k_{O2} among copper complexes and hemes; both synthetic and natural.[8c]

The $\%H_2O_2$ quantification and analysis of Tafel slopes derived from RRDE measurements provide a strong indication that the ORR goes through a stepwise mechanism (see Scheme 1). Herein O_2 is first reduced to H_2O_2, which in turn is further reduced to H_2O upon reaching the required potential. In this case the overall reaction will still yield a catalytic electron transfer number close to 4 in the O_2 mass-transport limited regime, as was established by KL and RRDE analysis. The onset potential of H_2O_2 reduction by Cu-tmpa is around 0.45 V vs. RHE, roughly 50 mV lower than that of O_2 reduction. The difference between onset potentials is small, which explains why $\%H_2O_2$ quickly lowers upon decreasing the potential. At low catalyst concentration a catalyst diffusion effect is observed and $\%H_2O_2$ is stable over a larger potential range before decreasing. This is expected as oxygen is a competitive inhibitor of H_2O_2 reduction. Peroxide will accumulate more at low catalyst concentrations, whereas it is more rapidly reduced at higher catalyst loadings while maintaining the same amounts of oxygen in solution. As both the ORR Tafel slope below 0.38 V and the Tafel slope for H_2O_2 reduction by Cu-tmpa are the same, it gives a strong indication the reduction of H_2O_2 to H_2O is rate determining in this potential window during the ORR. When FOWA is applied to determine the rate constant of the partial reduction of O_2 to H_2O_2, linearity of the catalytic current is only observed when applying the FOWA expression

corresponding to a first order catalytic system (see SI section 2.10). This shows that the partial reduction of O_2 to H_2O_2 is also first order in catalyst. The initial quantitative accumulation of hydrogen peroxide, the kink in the Tafel slope and its independence on the Cu-tmpa concentration, and the first order rate dependence in Cu-tmpa throughout point to two separate catalytic cycles, wherein H_2O_2 is readily replaced in the coordination sphere of copper (see Scheme 1).

Our findings contrast the previously proposed dinuclear mechanism for the ORR by Cu-tmpa using sacrificial reductants in acetone, where fast O_2 binding resulting in a copper superoxo species was followed by a slower dimerization step.[6a] Under aqueous electrochemical conditions, fast electron transfer and high proton mobility resulting in a fast PCET step most likely favours the formation of the hydroperoxo complex over dimerization.

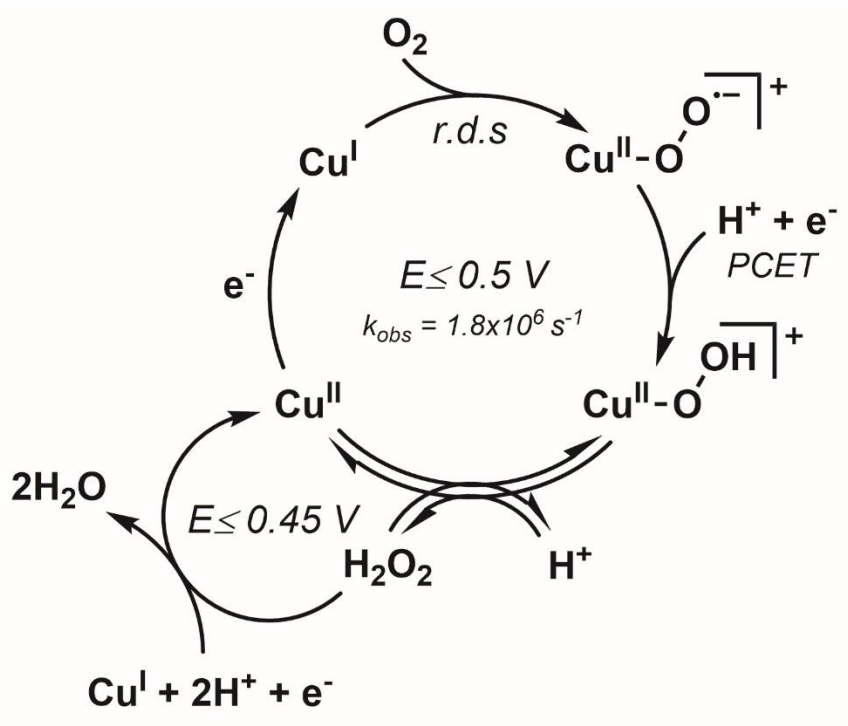

Scheme 1. Proposed stepwise mechanism for the electrocatalytic ORR in aqueous solution by Cu-tmpa. The tmpa ligand is not depicted for clarity.

To conclude, the electrocatalytic ORR activity of Cu-tmpa in neutral aqueous solution was quantified, revealing very fast kinetics and high TOFs. Application of the FOWA revealed that the TOF associated with the partial reduction of O_2 is very close to the O_2 binding constant with Cu-tmpa. This suggests that coordination of dioxygen to Cu^I is the rate determining step in the formation of peroxide. Additionally, we have shown that the ORR by Cu-tmpa goes through a stepwise type mechanism in aqueous solution, in which O_2 first undergoes 2-electron reduction to H_2O_2, followed by 2-electron reduction of H_2O_2 to H_2O. This stepwise mechanism was first mentioned as one of the possible mechanisms for Cu-tmpa by Asahi *et al.*, based on the ability of Cu-tmpa to catalyze the H_2O_2 reduction.[10a] However, until now there has been no direct evidence on whether a stepwise

reaction actually takes place during ORR. This work provides new insight the oxygen reduction reaction mediated by copper, and opens new possibilities towards the electrochemical synthesis of hydrogen peroxide relevant to energy conversion reactions, given that peroxide is an excellent candidate as a renewable fuel.

Acknowledgements

The European Research Council (ERC) is acknowledged for the funding of this project (ERC starting grant 637556 Cu4Energy to D. G. H. H.).

Keywords: copper • electrocatalysis • homogeneous catalysis • hydrogen peroxide • oxygen reduction

[1] a) H. A. Gasteiger, S. S. Kocha, B. Sompalli, F. T. Wagner, *Appl. Catal. B* **2005**, *56*, 9-35; b) O. Gröger, H. A. Gasteiger, J.-P. Suchsland, *J. Electrochem. Soc.* **2015**, *162*, A2605-A2622; c) A. Kongkanand, M. F. Mathias, *J. Phys. Chem. Lett.* **2016**, *7*, 1127-1137.

[2] E. I. Solomon, U. M. Sundaram, T. E. Machonkin, *Chem. Rev.* **1996**, *96*, 2563-2606.

[3] a) V. Soukharev, N. Mano, A. Heller, *J. Am. Chem. Soc.* **2004**, *126*, 8368-8369; b) N. Mano, V. Soukharev, A. Heller, *J. Phys. Chem. B* **2006**, *110*, 11180-11187; c) C. F. Blanford, R. S. Heath, F. A. Armstrong, *Chem. Commun.* **2007**, 1710-1712; d) J. A. Cracknell, K. A. Vincent, F. A. Armstrong, *Chem. Rev.* **2008**, *108*, 2439-2461; e) C. F. Blanford, C. E. Foster, R. S. Heath, F. A. Armstrong, *Faraday Discuss.* **2009**, *140*, 319-335; f) L. Rulíšek, U. Ryde, *Coord. Chem. Rev.* **2013**, *257*, 445-458.

[4] a) E. A. Lewis, W. B. Tolman, *Chem. Rev.* **2004**, *104*, 1047-1076; b) J. Serrano-Plana, I. Garcia-Bosch, A. Company, M. Costas, *Acc. Chem. Res.* **2015**, *48*, 2397-2406; c) S. Hong, Y.-M. Lee, K. Ray, W. Nam, *Coord. Chem. Rev.* **2017**, *334*, 25-42; d) C. E. Elwell, N. L. Gagnon, B. D. Neisen, D. Dhar, A. D. Spaeth, G. M. Yee, W. B. Tolman, *Chem. Rev.* **2017**, *117*, 2059-2107; e) L. M. Mirica, X. Ottenwaelder, T. D. P. Stack, *Chem. Rev.* **2004**, *104*, 1013-1046.

[5] a) P. Vasudevan, Santosh, N. Mann, S. Tyagi, *Transition Met. Chem. (London)* **1990**, *15*, 81-90; b) J. Zhang, F. C. Anson, *J. Electroanal. Chem.* **1992**, *341*, 323-341; c) J. Zhang, F. C. Anson, *J. Electroanal. Chem.* **1993**, *348*, 81-97; d) J. Zhang, F. C. Anson, *Electrochim. Acta* **1993**, *38*, 2423-2429; e) C. C. L. McCrory, X. Ottenwaelder, T. D. P. Stack, C. E. D. Chidsey, *J. Phys. Chem. A* **2007**, *111*, 12641-12650.

[6] a) S. Fukuzumi, H. Kotani, H. R. Lucas, K. Doi, T. Suenobu, R. L. Peterson, K. D. Karlin, *J. Am. Chem. Soc.* **2010**, *132*, 6874-6875; b) C. C. L. McCrory, A. Devadoss, X. Ottenwaelder, R. D. Lowe, T. D. P. Stack, C. E. D. Chidsey, *J. Am. Chem. Soc.* **2011**, *133*, 3696-3699; c) M. A. Thorseth, C. E. Tornow, E. C. M. Tse, A. A. Gewirth, *Coord. Chem. Rev.* **2013**, *257*, 130-139; d) S. Kakuda, R. L. Peterson, K. Ohkubo, K. D. Karlin, S. Fukuzumi, *J. Am. Chem. Soc.* **2013**, *135*, 6513-6522; e) M. L. Pegis, C. F. Wise, D. J. Martin, J. M. Mayer, *Chem. Rev.* **2018**, *118*, 2340-2391; f) S. Fukuzumi, Y.-M. Lee, W. Nam, *ChemCatChem* **2018**, *10*, 9-28.

[7] a) K. D. Karlin, J. C. Hayes, S. Juen, J. P. Hutchinson, J. Zubieta, *Inorg. Chem.* **1982**, *21*, 4106-4108; b) K. D. Karlin, S. Kaderli, A. D. Zuberbühler, *Acc. Chem. Res.* **1997**, *30*, 139-147; c) A. Wada, Y. Honda, S. Yamaguchi, S. Nagatomo, T. Kitagawa, K. Jitsukawa, H. Masuda, *Inorg. Chem.* **2004**, *43*, 5725-5735.

[8] a) K. D. Karlin, N. Wei, B. Jung, S. Kaderli, P. Niklaus, A. D. Zuberbuehler, *J. Am. Chem. Soc.* **1993**, *115*, 9506-9514; b) C. X. Zhang, S. Kaderli, M. Costas, E.-i. Kim, Y.-M. Neuhold, K. D. Karlin, A. D. Zuberbühler, *Inorg. Chem.* **2003**, *42*, 1807-1824; c) H. C. Fry, D. V. Scaltrito, K. D. Karlin, G. J. Meyer, *J. Am. Chem. Soc.* **2003**, *125*, 11866-11871.

[9] a) M. A. Thorseth, C. S. Letko, T. B. Rauchfuss, A. A. Gewirth, *Inorg. Chem.* **2011**, *50*, 6158-6162; b) M. A. Thorseth, C. S. Letko, E. C. M. Tse, T. B. Rauchfuss, A. A. Gewirth, *Inorg. Chem.* **2013**, *52*, 628-634.

[10] a) M. Asahi, S.-i. Yamazaki, S. Itoh, T. Ioroi, *Dalton Trans.* **2014**, *43*, 10705-10709; b) M. Asahi, S.-i. Yamazaki, S. Itoh, T. Ioroi, *Electrochim. Acta* **2016**, *211*, 193-198.

[11] a) C. Costentin, S. Drouet, M. Robert, J.-M. Savéant, *J. Am. Chem. Soc.* **2012**, *134*, 11235-11242; b) R. M. Bullock, A. M. Appel, M. L. Helm, *Chem. Commun.* **2014**, *50*, 3125-3143; c) A. M. Appel, M. L. Helm, *ACS Catalysis* **2014**, *4*, 630-633; d) E. S. Rountree, B. D. McCarthy, T. T. Eisenhart, J. L. Dempsey, *Inorg. Chem.* **2014**, *53*, 9983-10002.

[12] a) C. Costentin, J.-M. Savéant, *ChemElectroChem* **2014**, *1*, 1226-1236; b) D. J. Wasylenko, C. Rodríguez, M. L. Pegis, J. M. Mayer, *J. Am. Chem. Soc.* **2014**, *136*, 12544-12547; c) D. J. Martin, B. D. McCarthy, E. S. Rountree, J. L. Dempsey, *Dalton Trans.* **2016**, *45*, 9970-9976; d) C. Costentin, D. G. Nocera, C. N. Brodsky, *Proc. Natl. Acad. Sci.* **2017**, *114*, 11303-11308; e) C. Costentin, J.-M. Savéant, *J. Am. Chem. Soc.* **2017**, *139*, 8245-8250.

[13] a) N. D. Schley, J. D. Blakemore, N. K. Subbaiyan, C. D. Incarvito, F. D'Souza, R. H. Crabtree, G. W. Brudvig, *J. Am. Chem. Soc.* **2011**, *133*, 10473-10481; b) D. G. H. Hetterscheid, C. J. M. van der Ham, O. Diaz-Morales, M. W. G. M. Verhoeven, A. Longo, D. Banerjee, J. W. Niemantsverdriet, J. N. H. Reek, M. C. Feiters, *Phys. Chem. Chem. Phys.* **2016**, *18*, 10931-10940; c) D. G. H. Hetterscheid, *Chem. Commun.* **2017**, *53*, 10622-10631; d) B. van Dijk, J. P. Hofmann, D. G. H. Hetterscheid, *Phys. Chem. Chem. Phys.* **2018**, *20*, 19625-19634.

[14] P. A. Malachesky, L. S. Marcoux, R. N. Adams, *The Journal of Physical Chemistry* **1966**, *70*, 4068-4070.

[15] M. L. Pegis, B. A. McKeown, N. Kumar, K. Lang, D. J. Wasylenko, X. P. Zhang, S. Raugei, J. M. Mayer, *ACS Cent. Sci.* **2016**, *2*, 850-856.